

# *mab-2* encodes RNT-1, a *C. elegans* Runx homologue essential for controlling cell proliferation in a stem cell-like developmental lineage

Rachael Nimmo<sup>1</sup>, Adam Antebi<sup>2</sup> and Alison Woollard<sup>1,\*</sup>

<sup>1</sup>Genetics Unit, Department of Biochemistry, University of Oxford, South Parks Road, Oxford OX1 3QU, UK

<sup>2</sup>Huffington Center on Ageing and Department of Molecular and Cellular Biology, Baylor College of Medicine, One Baylor Plaza, Room M-320, Houston TX 77030, USA

\*Author for correspondence (e-mail: alison.woollard@bioch.ox.ac.uk)

Accepted 15 September 2005

Development 132, 5043-5054

Published by The Company of Biologists 2005

doi:10.1242/dev.02102

## Summary

In this report, we demonstrate that *C. elegans mab-2* mutants have defects in the development of a male-specific sense organ because of a failure in the proliferation of the stem cell-like lateral hypodermal (seam) cells. We show, by positional cloning, that *mab-2* encodes RNT-1, the only *C. elegans* member of the Runx family of transcriptional regulators, which are postulated to act both as oncogenes and tumour suppressors in mammalian cells. Importantly, we find that *rnt-1* is a rate-limiting regulator of seam cell proliferation in *C. elegans*, as overexpression of *rnt-1* at particular developmental stages is capable of driving extra cell divisions, leading to seam cell hyperplasia. Loss of *rnt-*

*1* is correlated with upregulation of *cki-1*, a CDK inhibitor. Deregulated expression of Runx genes in humans is associated with various cancers, particularly leukaemias, suggesting a conserved role for Runx genes in controlling cell proliferation during development, especially in stem cell lineages. *C. elegans* is therefore an important model system for studying the biology, and oncogenic potential, of Runx genes.

Key words: *Caenorhabditis elegans*, Runx genes, Cell proliferation, Male tail development

## Introduction

During development, it is essential for cell division to be properly regulated in time and space so that the correct number of cells are produced in the appropriate location at the required time. These controls ensure that the developmental process culminates in an organism of the appropriate size and complexity. Failure of such controls over cell proliferation can result in tumourigenesis in many metazoan organisms.

Coordination of cell division with growth and differentiation is achieved, at least in part, through the integration of extracellular signals during the G1 phase of the cell cycle (Zhu and Skoultschi, 2001). Cells respond to such signals by either advancing into, or withdrawing from, the next division cycle. Ultimately, signals impinge on the cell-cycle machinery intrinsic to each cell, composed of cyclin-dependent kinases (CDKs) and CDK inhibitors (CDKIs) among other factors.

During *C. elegans* development, cell divisions are almost completely invariant and well characterised (Sulston and Horvitz, 1977; Sulston et al., 1983). The effects of mutations on cell proliferation during development can thus be analysed at high resolution. Normal development gives rise to 959 somatic nuclei in the wild-type hermaphrodite and 1031 in the male. As an organism develops, individual cells must either continue to divide (proliferate) or differentiate and adopt a specialised function. Many cell lineage mutants have been identified that do not produce the correct number of cells, and

these may be subdivided in various ways. For example, some mutants are defective in cell division itself, others have defects in the timing of particular cell divisions and a third group have defects in the polarity, or asymmetry, of divisions, leading to fate changes that may influence the choice between subsequent proliferation and differentiation.

The *C. elegans* male tail is an excellent system for genetic studies because this sensory organ is dispensable for viability. The male tail includes the proctodeum, which houses two sclerotized spicules and associated musculature used for the transfer of sperm, and a cuticular fan containing sensory rays used to locate the hermaphrodite vulva during mating (Sulston et al., 1980). The male tail forms from postembryonic divisions of male-specific blast cells and extra divisions of posterior lateral hypodermal (seam) cells and is particularly sensitive to alterations in cell number, which result in recognisable developmental defects. A well-defined set of mutants, the Mab (male abnormal) mutants, have a range of defects in male tail development (Hodgkin, 1983). *mab-2* mutants have variable defects in sensory ray formation (Hodgkin, 1983).

In this report, we show that the *mab-2* phenotype is caused by reduced proliferation of seam cells in both sexes, resulting in the loss of V and T derived rays in males. We show that *mab-2* encodes a Runt domain transcription factor, RNT-1, which is similar to Runx proteins from other species. In humans, mis-expression of Runx genes is associated with

leukaemias and other cancers (reviewed by Coffman, 2003). Most importantly, we find that overexpression of *mab-2/rnt-1* in *C. elegans* causes seam cell hyperplasia, suggesting that *mab-2/rnt-1* is a conserved factor required to control the extent of cell proliferation during the development of metazoan organisms.

## Materials and methods

### Strains and *C. elegans* maintenance

All *C. elegans* strains were derived from the wild-type Bristol strain N2. Routine maintenance of worms and genetic manipulations were performed as described previously (Sulston and Hodgkin, 1988). The *him-5(e1490)* and *him-8(e1489)* alleles were used where necessary to generate a high proportion of males. Phenotypic analyses were carried out using a Zeiss Axiophot microscope fitted with DIC and fluorescence optics as appropriate. Worms were anaesthetised on 2% agarose pads as previously described (Sulston and Hodgkin, 1988). Statistical analysis of quantitative data was performed using the unpaired two-tailed heteroscedastic *t*-test function of Microsoft Excel.

### Growth curves

Well fed young adult hermaphrodites were picked to a fresh plate and allowed to lay eggs for 1 hour at 20°C. Hatched larvae were then measured after 1, 2, 3 and 4 days growth at 20°C by mounting on 2% agarose pads containing anaesthetic and measuring the length of each worm using Axiovision software.

### Mapping

*mab-2* was originally mapped to the region between *dpy-5* (0.00, cloned map position) and *unc-13* (2.06, cloned map position) on LG1 (Jonathan Hodgkin, personal communication). Further mapping revealed *mab-2* to be to the right (or very close to the left) of *unc-40* (0.32, cloned map position) and to the left (or very close to the right) of *air-2* (0.49, cloned map position). The order of the nine cosmids in this region (left to right) is as follows: T19B4 (contains *unc-40*)–C04F1–F56H1–T22E7–B0414–C32F10–F33D11–C34G6–B020 7 (contains *air-2*). Confirmed single nucleotide polymorphism (SNP) markers assayable by restriction enzyme analysis, which differ between the Bristol N2 strain and the Hawaiian strain CB4856, are available for cosmids C04F1 (C04F1:3815) and C34G6 (C34G6:15466). Recombinants were picked from the heterozygote *dpy-5 mab-2 unc-13/CB4856*. Ten out of 10 Dpy Mab non-Unc recombinants were found to be wild type for SNP C04F1:3815, and nine out of nine Unc non-Mab non-Dpy recombinants were found to be Hawaiian for SNP C04F1:3815. These data indicate that *mab-2* is to the right of C04F1:3815 (or very close to the left). Four out of four Unc Mab non-Dpy recombinants were found to be wild type for SNP C34G6:15466, and seven out of nine Unc non-Mab non-Dpy recombinants were found to be Hawaiian for SNP C34G6:15466. These data indicate that *mab-2* lies to the left of C34G6:15466. The five cosmids between C04F1 and C34G6 were tested for rescue of *mab-2(e1241)*, and cosmid B0414 was found to rescue the mutant phenotype completely. Oligos used for SNP C04F1:3815 were RN3 (5'GGATTTATCAGCGATGGATCAG) and RN4 (5'CATTGCCA-GAGGGATTGAAC), yielding a 784 bp PCR product, cut by *Tsp45I* in N2 to give bands of 490 bp and 294 bp. For SNP, C34G6:15466 oligos were RN5 (5'GCAGTTCGGTGAGTGGATTG) and RN6 (5'GGTAGCAGATGTTTACACAGTC), yielding a 992 bp PCR product, cut by *TaqI* in N2 to give bands of 42 bp, 225 bp, 276 bp and 449 bp, and in CB4856 to give bands of 25 bp, 42 bp, 225 bp, 251 bp and 449 bp. These differences could be easily resolved on a 2% agarose gel.

### Lineage analysis

Worms were mounted on 2% agarose pads (Sulston and Hodgkin,

1988) in 2  $\mu$ l of M9 to which a smear of OP50 bacteria had been added and mixed. A 12 $\times$ 12 mm coverslip was gently lowered onto the worm and the divisions of the seam cells were observed using Nomarski DIC optics and a 63 $\times$  oil immersion objective (Zeiss) over a period of 18–20 hours.

### Transgenic worms

Plasmids were injected into the syncytial gonad of young adult hermaphrodite worms at a concentration of 30 ng/ $\mu$ l as described (Mello and Fire, 1995), along with the *rol-6* transformation marker (at 50–100 ng/ $\mu$ l). Rol progeny were picked and stable lines selected for analysis. Several lines were generated for each construct.

### Transformation rescue of *rnt-1*

Cosmid B0414 was found to rescue the *rnt-1(e1241)* mutant phenotype. Subclones were generated to test for single gene rescuing activity and a fragment containing the single gene B0414.2 was found to rescue. This subclone was generated by PCR amplification from cosmid B0414 and TA cloned into TOPOXL (Invitrogen) in two halves using oligos RN64 and RN83 (5' half) and RN68 and RN82 (3' half). The 3' half (7902 bp) was then subcloned into the 3' end of the 5' half (8428 bp) using *XbaI* and *BglII* to generate the full-length B0414.2 genomic clone pAW258. The rescued strain referred to in this report carrying the whole cosmid B0414 is AW44 [*rnt-1(e1241); him-5(e1490); ouEx15[B0414 + rol-6]*] and the rescued strain referred to in this report carrying the single gene B0414.2 (*rnt-1*) is AW68 [*rnt-1(e1241); him-5(e1490); ouEx17[B0414.2 + rol-6]*].

### Sequencing of *rnt-1* alleles

Primers were used to amplify *rnt-1* coding sequences from appropriate mutant worms for sequencing using the high-fidelity Expand DNA polymerase (Roche). PCR from worms was performed as described previously (Williams, 1995). Sequences (both strands) of at least two independent PCR products were analysed using Pairwise Alignment in BioEdit.

### GFP reporter constructs

A *rnt-1* translational GFP fusion construct was made using pPD vectors kindly supplied by the Fire Lab (Stanford University). All constructs were verified by sequencing. To make *rnt-1::GFP*, GFP from pPD119.16 was excised using *SmaI* and inserted into the *StuI* site at the 3' end of the 3' *rnt-1* clone. Then, this GFP-tagged 3' clone was inserted into the 3' end of the 5' clone using *XbaI* and *BglII* as above, to generate a full-length genomic GFP-tagged rescuing construct, pAW260. The rescued strain referred to in this report carrying this *rnt-1::GFP* translational fusion is AW109 (*rnt-1(e1241); him-5(e1490); ouEx26[rnt-1::GFP + rol-6]*). *rnt-1(ok351) him-5(e1490)* was crossed into the *scm::GFP* seam cell reporter strain (JR667) to generate the strain AW58, into a *myo-3::GFP* muscle cell reporter (strain PD4251) to generate the strain AW106 and into a *cki-1::GFP* reporter (strain VT825) to generate the strain AW148.

### Heat-shock constructs

A full-length *rnt-1* cDNA construct was generated by PCR from a *C. elegans* cDNA library (gift from R. Barstead, Oklahoma University) and used to generate two *hsp-16* driven constructs (F primer 5'GCTAGCCAGTGCTGGAAGTATTCTGGG, RN87; R primer 5'GAGCTCCTGAAGAGGTAGGAAACAATTGAG, RN88, product 994bp). pAW261 consists of the *rnt-1* cDNA cloned into pPD49.78 (*hsp16-2* driven) as a *NheI-SacI* fragment. pAW262 consists of *rnt-1* cDNA cloned into pPD49.83 (*hsp16-41* driven) as a *NheI-SacI* fragment. The transgenic line generated for pAW261 described in this study is AW87 (*him-5(e1490); ouEx19[hsp16-2::rnt-1 + rol-6<sup>+</sup>]*). AW87 was crossed into the *scm::GFP* seam cell reporter strain to generate the strain AW102 and into *rnt-1(e1241); him-5(e1490)* to generate the strain AW103. A transgenic line was also constructed carrying pAW262 as well as an *elt-2::GFP* intestinal reporter (gift from Joel Rothman, University of California, Santa Barbara) by co-

injecting both reporters in addition to the *rol-6* transformation marker, to generate the strain AW100 (*him-5(e1490); ouEx23[hsp16-41::rnt-1 + elt-2::GFP + rol-6*).

### Heat-shock experiments

Worms were staged by bleaching gravid adult hermaphrodites to produce a pure egg population that was then allowed to hatch in the absence of food to produce a synchronous population of arrested L1 stage animals (Sulston and Hodgkin, 1988). These animals were then re-fed on OP50 seeded NGM plates and heatshocked at 33°C for 1 hour at different larval stages.

### RNAi

PCR primers, including T7 or T3 RNA polymerase promoter sites were designed to be specific for *rnt-1*, and to amplify 504 bp of mostly exonic sequence (F primer 5'ATTAACCCTCACTAAAGGTTACG-GTTGATGGACC, RN84; R primer 5'AATACGACTCACTATAGC-GGAGAAGAACTATTCG, RN85). Primers specific for *cki-1* amplified 602 bp (F primer 5'ATTAACCCTCACTAAAGGTTCTTC-TGCTCGTTCGTTGCC, RN90; R primer 5'AATACGACTCACTA-TAGGAGAGCATGAAGATCGAGTTCG, RN91). dsRNA was synthesised directly from gel-purified PCR product as previously described (Fire et al., 1998) and injected into young adult hermaphrodites at a concentration of ~1 mg/ml. Injected worms were transferred to fresh plates 6 hours following injection and thereafter every 24 hours for 3 days.

## Results

### *mab-2* mutants have missing V and T lineage derived rays

*mab-2(e1241)* mutant males have a variable missing ray phenotype, typically lacking 5 rays from each side of the tail (Fig. 1, Fig. 2D). The phenotype is identical in two other alleles of *mab-2*, *os11* and *os58* [kind gifts from Hitoshi Sawa (Fig.

2 and data not shown)]. Both V and T derived rays are variably missing. We also noticed a low (5-10%) penetrance ray fusion phenotype in *mab-2* males (Fig. 1E). Ray fusions may simply be a consequence of missing intervening rays. However, it is also possible that *mab-2* has some downstream function in specifying ray identity, separate from its function in specifying ray number.

To examine the cellular basis of the missing ray phenotype, we examined tail development using the *ajm-1::GFP* reporter (Strain SU93), which marks adherens junctions and shows the outlines of male tail precursor cells derived from the posterior seam. We found fewer ray precursor cells in *mab-2* mutants compared with wild type (Fig. 1), indicating either a failure of cell proliferation or a cell fate transformation in V5, V6 and T lineages.

### *mab-2* encodes RNT-1, a member of the Runx group of transcription factors

We mapped *mab-2* to the centre of chromosome 1, between *unc-40* and *air-2*, using three-factor crosses (see Materials and methods). SNP mapping was then used to further map *mab-2* to a region spanned by seven cosmids (see Materials and methods) and these cosmids were tested for rescuing activity. The cosmid B0414 was found to completely rescue the phenotype of *mab-2* mutant worms, and a subclone including the full ORF of only one gene, B0414.2, was subsequently found to provide all of this rescuing activity (Fig. 2A). Examination of the sequence of B0414.2 revealed it to encode a transcription factor of the Runx family, members of which include human *RUNX1*, *RUNX2*, *RUNX3* and *Drosophila runt* and *lozenge* (Fig. 2C). B0414.2 has been given the name *RNT-1* in Wormbase

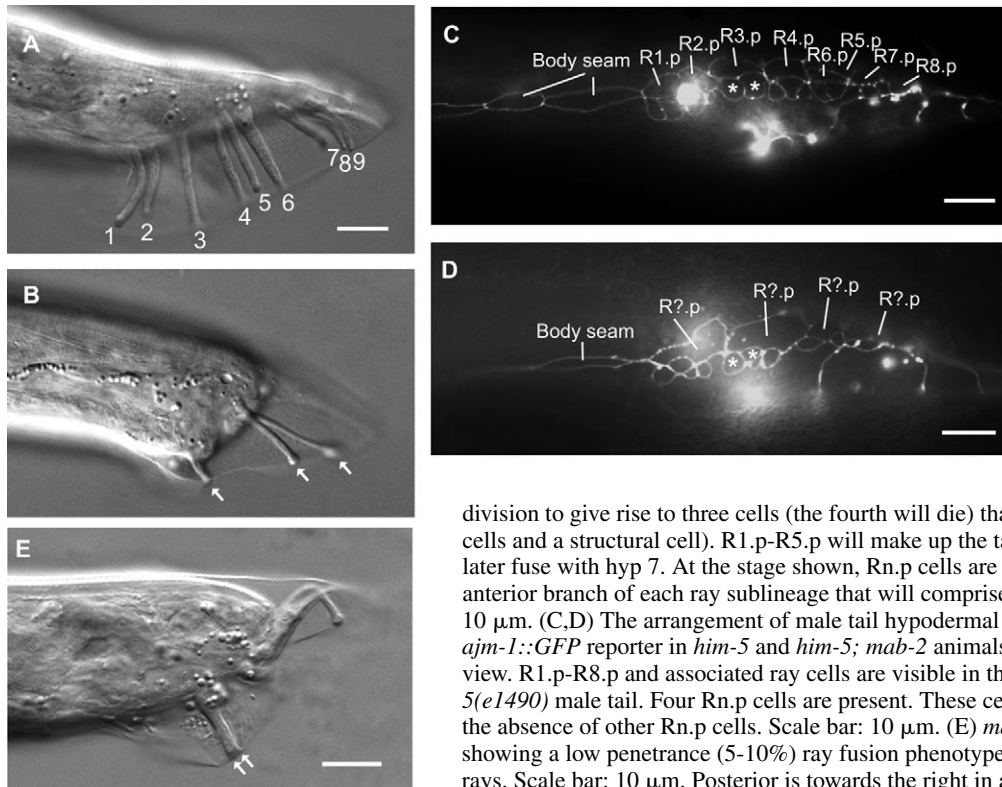


**Fig. 1.** Loss of V and T rays in *mab-2* mutants. (A) *him-5(e1490)* male tail, wild-type appearance. Lateral view. Nine sensory rays are visible on this side of the animal. Rays 1-6 are derived from the V lineage and rays 7-9 are T-lineage derived. Scale bar: 10  $\mu$ m. (B) *mab-2(e1241); him-5(e1490)* male tail. Only three rays are present (white arrows). Scale bar: 10  $\mu$ m. During execution of the ray sublineages, the ray precursor cells (R1-R9) divide to give a posterior hypodermal cell (R1.p-R9.p) and an anterior daughter that will go on to undergo two rounds of

division to give rise to three cells (the fourth will die) that will make up the ray (two neuronal cells and a structural cell). R1.p-R5.p will make up the tail seam (set), whereas R6.p-R9.p will later fuse with hyp 7. At the stage shown, Rn.p cells are visible (labelled), as are cells from the anterior branch of each ray sublineage that will comprise each ray (white asterisks). Scale bar: 10  $\mu$ m. (C,D) The arrangement of male tail hypodermal cells in L4 males visualised using the *ajm-1::GFP* reporter in *him-5* and *him-5; mab-2* animals. (C) *him-5(e1490)* male tail. Lateral view. R1.p-R8.p and associated ray cells are visible in this focal plane. (D) *mab-2(e1241); him-5(e1490)* male tail. Four Rn.p cells are present. These cells have enlarged to fill the gap left by the absence of other Rn.p cells. Scale bar: 10  $\mu$ m. (E) *mab-2(e1241); him-5(e1490)* male showing a low penetrance (5-10%) ray fusion phenotype. Two white arrows indicate the fused rays. Scale bar: 10  $\mu$ m. Posterior is towards the right in all panels.

(<http://www.wormbase.org/>) and is the only Runx orthologue present in the worm genome.

A deletion allele of *rnt-1* is available from the *C. elegans* Knockout Consortium (Oklahoma, USA, allele *ok351*). We found that this allele fails to complement the male tail

phenotype of *mab-2(e1241)* (Fig. 2A), demonstrating that *mab-2* and *rnt-1* are allelic. For simplicity we will henceforward refer to *mab-2* as *rnt-1*. The male tail phenotype of the *rnt-1* deletion allele, *ok351*, is indistinguishable from *e1241*, with the same number of

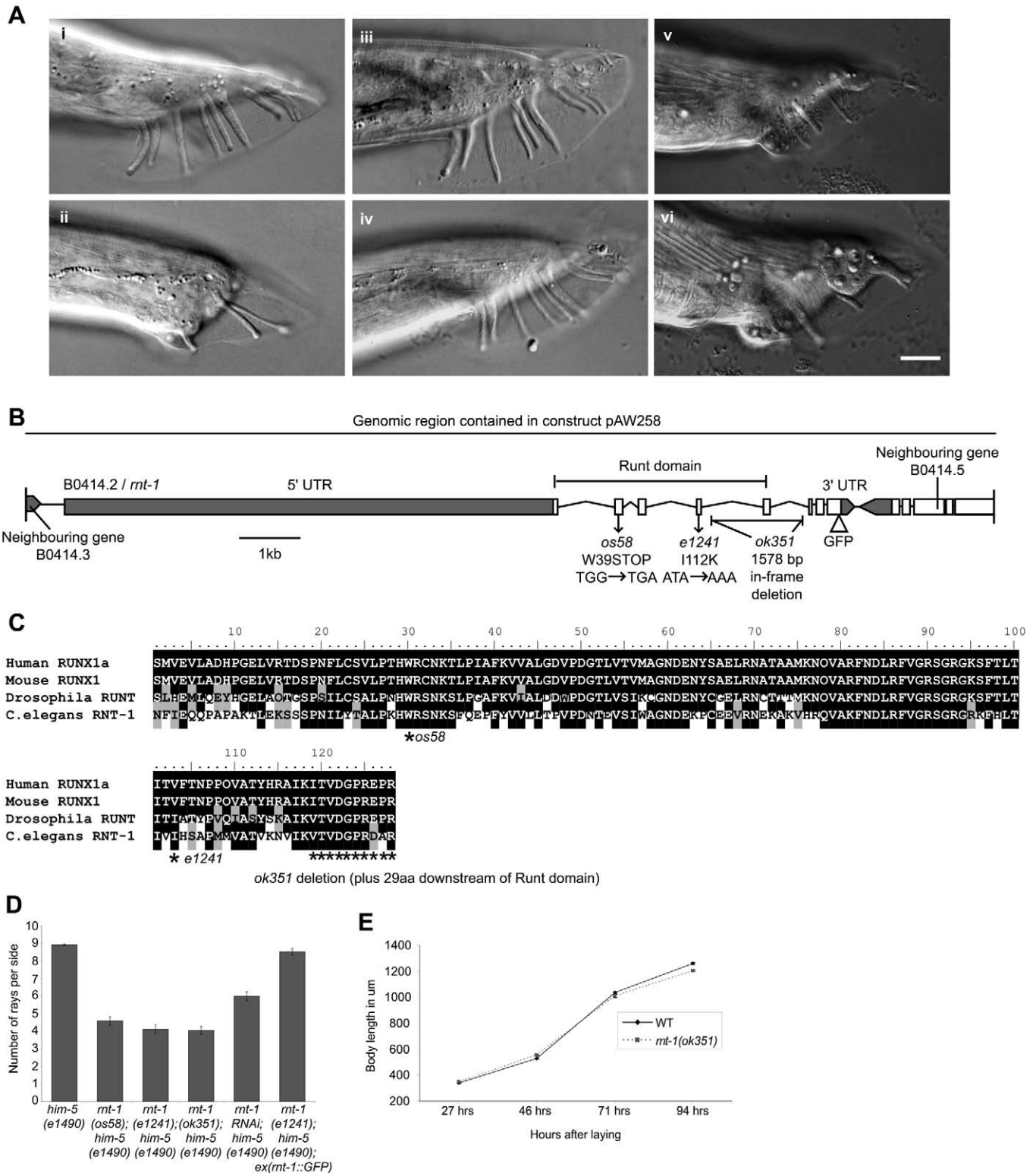


Fig. 2. See next page for legend.

rays, on average, being missing from each side of the tail (Fig. 2D).

The molecular nature of the lesions associated with these alleles are shown in Fig. 2. The mutation in *e1241* results in a single amino acid substitution, I112K, in a conserved part of the DNA-binding domain, changing a hydrophobic residue into a hydrophilic one. *os58* contains a premature stop codon near the N terminus of the protein (H. Kagoshima, personal communication). This allele is therefore a likely null allele and has the same male tail phenotype as *e1241* and *ok351* (Fig. 2D). The trans-heterozygote *os58/e1241* is indistinguishable from a *e1241* or *os58* homozygote (Fig. 2A; data not shown). The deletion in *ok351* removes 10 amino acids from the Runt domain plus an additional 29 amino acids downstream, but leaves the reading frame intact.

Silencing *rnt-1* using RNA interference (RNAi) also gave rise to males with missing rays, similar to the loss of function alleles described (Fig. 2D). There was a small but significant amount of embryonic lethality associated with *rnt-1* RNAi (18% embryonic lethality at 25°C in *him-8(e1489)*; *rnt-1(RNAi)* animals compared with 3.6% embryonic lethality in *him-8(e1489)* animals kept at 25°C but not subjected to RNAi:

**Fig. 2.** *mab-2* encodes RNT-1, a Runx transcription factor. (A) (i) *him-5(e1490)* male tail. (ii) *mab-2(e1241)*; *him-5(e1490)* male tail. (iii) *mab-2(e1241)*; *him-5(e1490)*; *ouEx15[B0414 + rol-6]* male tail. Wild-type appearance is restored using this cosmid. (iv) *mab-2(e1241)*; *him-5(e1490)*; *ouEx17[B0414.2 + rol-6]* male tail. Wild-type appearance is restored using the single gene *B0414.2*, encoding the Runx transcription factor *rnt-1*. (v) male tail from a *e1241/ok351* trans-heterozygote, showing that these two alleles fail to complement each other. (vi) Male tail from a *e1241/os58* trans-heterozygote, again showing non-complementation between the two alleles. Scale bar: 10 µm. Posterior is towards the right in all panels. (B) Schematic representation showing the genomic structure of the *rnt-1* gene, the nature and position of the mutations in *e1241* and *os58* alleles, and the deletion in *ok351*. The genomic region shown corresponds to the region cloned in the rescuing construct pAW258. The position of the GFP insertion in pAW260 is also indicated. (C) Alignment of Runx genes from various species showing the conserved DNA-binding domain. Identical amino acids are shown in black; similar amino acids are in grey. The Runt domain of *rnt-1* (Accession Number O01834) is 51% similar to *Drosophila Runt* (Accession Number CAA39817), 50% similar to human *RUNX1* (Accession Number NP\_001745) and 50% similar to mouse *Runx1* (Accession Number Q03347). Sequence alignments were performed using ClustalW and processed using BioEdit software. The nature of the mutations in *e1241*, *os58* and *ok351* animals are indicated with asterisks. The *ok351* deletion removes 10 amino acids of the Runt domain plus 29 amino acids downstream in an in-frame deletion. (D) Bar chart showing a quantitative analysis of ray number in wild-type ( $n=33$ ), *rnt-1(os58)* ( $n=37$ ), *rnt-1(e1241)* ( $n=31$ ), *rnt-1(ok351)* ( $n=35$ ), *rnt-1(RNAi)* ( $n=28$ ) and *rnt-1(e1241)*; *ouEx26[rnt-1::GFP+rol-6<sup>+</sup>]* ( $n=35$ ) males. Ray number in all three *rnt-1* alleles, as well as in *rnt-1(RNAi)* males is significantly different from wild type ( $P<0.0001$ ). Ray number in *rnt-1(e1241)*; *Ex[rnt-1::GFP]* males is not significantly different from wild type ( $P>0.05$ ), indicating rescue. Error bars represent the standard error of the mean. (E) Graph showing length growth curves of wild-type and *rnt-1(ok351)* animals. There is no significant reduction in the length of *ok351* animals compared with wild-type animals until the worms have reached adulthood, 4 days after eggs were laid. A ~5% decrease in *ok351* body length is seen at this time point ( $n=33$  for wild type, 30 for *ok351*,  $P<0.00001$ ). Error bars represent the s.e.m.

14.4% lethality is thus attributable to the effects of *rnt-1* RNAi). A similar amount of embryonic lethality is seen in *rnt-1(os58)* animals [50% embryonic lethality in *rnt-1(os58)*; *him-5(e1490)* animals kept at 25°C compared with 38% embryonic lethality in *him-5(e1490)* animals alone kept at 25°C: 12% lethality is thus associated with the *os58* allele]. None of the other *rnt-1* alleles displays any significant embryonic lethality, so it is possible that those alleles, including the deletion allele *ok351*, are non-null. *rnt-1(os11)* was found to be largely inviable at 25°C, with much reduced fertility, but the lesion in *os11* animals appears to be a large deletion also affecting a neighbouring gene (R.N. and A.W., unpublished), which known from genome-wide RNAi screens to be essential (Kamath et al., 2003).

*rnt-1* hermaphrodites have no defects at the gross morphological level, except a slight (5%) reduction in body length at adulthood (Fig. 2E). The slight reduction in body length is similar in all alleles tested (data not shown). We noticed that the reduction in body length was more pronounced in *rnt-1* worms recovering from starvation, and these worms were found to be very sick (data not shown), suggesting that *rnt-1* may have some function in stimulating growth following starvation. No other defects were observed in any of the *rnt-1* mutant strains tested, or in *rnt-1(RNAi)* animals.

### Seam cell number is reduced in *rnt-1* animals

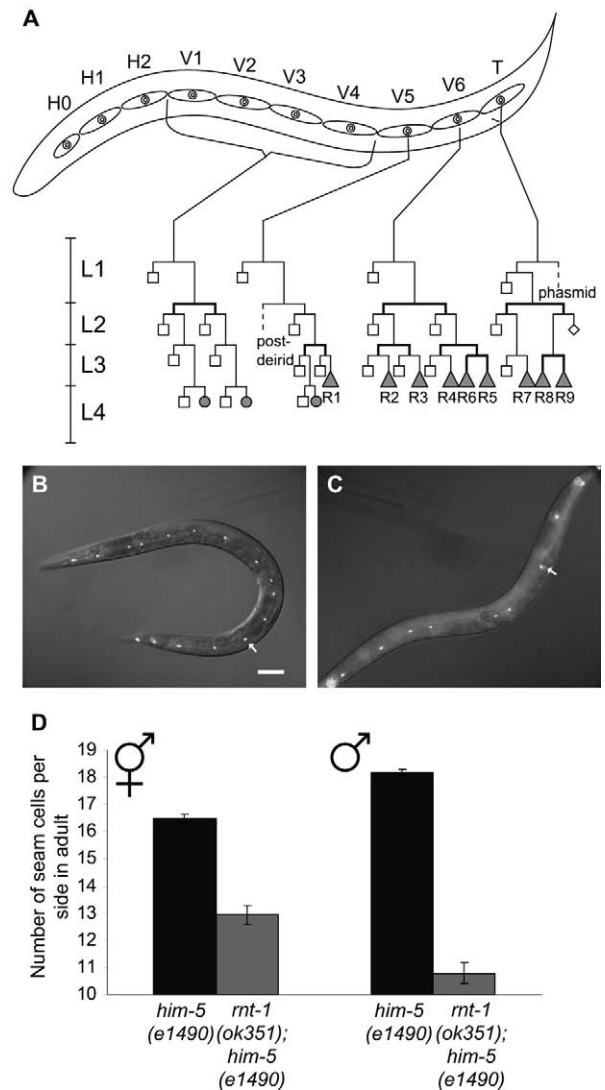
In wild-type males, the rays are generated by seam cells. Seam cell divisions in both sexes provide hypodermal nuclei and a postdeirid neuroblast (Sulston and Horvitz, 1977). In males, extra divisions in the posterior seam cells V5, V6 and T and subsequent specification of ray neuroblasts result in generation of the 18 rays.

We analysed the number of seam cells in *rnt-1* mutants using the seam cell marker *scm::GFP*. Wild-type adult hermaphrodites usually contain 16 seam cells on each side of the animal at the end of development, derived from the 10 embryonically derived blast cells H0, H1, H2, V1-V6 and T (Fig. 3). *rnt-1* mutant hermaphrodites contain fewer, typically 13 (Fig. 3). Male *rnt-1* mutant worms also contain fewer seam cells, typically 11, compared with 18 in wild type (Fig. 3). This indicates that *rnt-1* activity is required in both males and hermaphrodites for either seam cell proliferation or differentiation, and that this is the basis of the male tail phenotype, as sensory rays are generated from posterior seam cells. Seam cells in *rnt-1* animals (albeit reduced in number) fuse normally in L4 (visualised with *ajm-1::GFP*, data not shown), indicating that they maintain the correct fate. In hermaphrodites, seam cells are responsible for the formation of alae, cuticular ridges on the surface of the worm (Sulston and Horvitz, 1977). Despite the lack of seam cells in *rnt-1* mutants, alae do not appear to be defective (data not shown), again indicating that correct seam cell fate is maintained in the remaining seam cells.

### *rnt-1* is expressed in seam cells

The expression pattern of a rescuing translational *rnt-1::GFP* fusion construct is shown in Fig. 4. *rnt-1::GFP* is visibly expressed in the nuclei of seam cells in embryos from around 260 minutes post fertilisation, just after the time at which seam cell are formed. Seam cell expression in both males and hermaphrodites is visible during all developmental stages, but

**Fig. 3.** *rnt-1* mutants have fewer seam cells. (A) Lineage diagram showing V and T lineage divisions in wild-type males. Seam cells are indicated by circles, *hyp7* nuclei by squares, glial and neuronal cells by diamonds, and ray precursor cells by triangles. Proliferative divisions are in bold. The broken lines indicate parts of the lineage omitted for simplicity. The V and T lineages of the male are identical to those of the hermaphrodite until the end of L2. Divisions are asymmetric and stem cell like, with the anterior daughter adopting the syncytial fate (fusing with the hypodermal cell *hyp7*) and the posterior daughter adopting the proliferative fate (Sulston and Horvitz, 1977). An exception to this division pattern is at the beginning of L2, when an extra symmetrical division occurs in both sexes in V1-V4, V6 and T, resulting in an increase in seam cell number. In hermaphrodites, asymmetric divisions then continue, whereas in males V5-, V6- and T-derived cells undergo extra symmetrical, proliferative divisions at the beginning of L3 in order to generate nine ray precursor cells (R1-R9) (Sulston and Horvitz, 1977). Male-specific ray sub-lineages then give rise to nine similar sets of neuronal-like cells (including a structural cell) on each side of the animal, corresponding to the nine rays found on each side of the male tail, as well as nine hypodermal-like cells (Rn.p cells). The characteristic ray sensilla are formed by retraction of the hypodermis surrounding the ray cell groups, leaving finger-like protrusions embedded in the cuticular fan. (B,C) Seam cells in adult hermaphrodites visualised using the *scm::GFP* reporter. This reporter shows all seam cell nuclei (white arrows indicate one such nucleus in each panel) present along the length of the animal. (B) *him-5(e1490)*. All 16 seam cells are present. (C) *rnt-1(ok351); him-5(e1490)* adult hermaphrodite. Fewer seam cells are present, 11 in this specimen. The most anterior seam cell is not visible in this photograph. Scale bar in B: 70  $\mu$ m for B,C. (D) Graph showing a quantitative analysis of seam cell number in *him-5(e1490)* ( $n=30$ ) and *rnt-1(ok351); him-5(e1490)* ( $n=32$ ) adult hermaphrodites and males ( $n=30$  for *him-5(e1490)* males;  $n=28$  for *rnt-1(ok351); him-5(e1490)* males). There is a significant difference between wild-type and *rnt-1* seam cell number in both hermaphrodites and males ( $P<0.0001$ ). Error bars represent the s.e.m. The y-axis starts at 10 to reflect the number of seam cells present at hatching, as it is only post-embryonic divisions that are affected in *rnt-1* mutants.



is particularly strong until late L2. In males, *rnt-1::GFP* is expressed additionally in seam cell derived ray precursor cells and ray sublineages. *rnt-1::GFP* is also expressed transiently in body wall muscle nuclei from late embryogenesis until the end of L2 (Fig. 4). We could find no obvious phenotype associated with expression of *rnt-1* in body wall muscle. Both the number and arrangement of body wall muscle nuclei (assayed using a *myo-3::GFP* reporter) in *rnt-1* mutants appears normal (data not shown). We did not observe *rnt-1::GFP* expression in any other cell types. Expression of *rnt-1* has been previously reported in intestinal cells (Nam et al., 2002), but we did not find any intestinal expression using our rescuing GFP reporter construct, nor did we observe any intestinal defects in *rnt-1* mutant alleles or *rnt-1(RNAi)* animals. Our rescuing GFP reporter contains the endogenous *rnt-1* 3'UTR that was absent from the reporter described by Nam et al. It is possible that this difference in reporters accounts for the slight difference in the *rnt-1* expression pattern observed.

### ***rnt-1* is specifically required for seam cell proliferation, not cell fate determination**

One possible interpretation of our data could be that *rnt-1* is required for cell fate determination, rather than cell

proliferation per se. For example, controls acting on the polarity of seam cell divisions can influence cell proliferation. The seam cells normally undergo polarized divisions during larval development, such that the posterior daughters (*Vn.p*) adopt the seam cell (proliferative) fate and the anterior daughters (*Vn.a*) adopt the non-proliferative, syncytial fate, fusing with the hypodermal syncytium *hyp7* (Sulston and Horvitz, 1977). It is therefore possible that *rnt-1* mutants could fail to maintain seam cell number if, at particular seam cell divisions, the posterior daughter adopted the hypodermal fate like its anterior neighbour. Alternatively, divisions could fail as a direct result of a failure to enter or progress through the cell cycle. In order to distinguish between these two possibilities, we performed a detailed lineage analysis of seam cell divisions in *rnt-1* mutants. A lineage trace of seam cell divisions in a *rnt-1(ok351)* hermaphrodite from late L1 up to mid L3 is shown in Fig. 5B. Various seam division failures are evident in this animal, as discussed in the figure legend. A *rnt-1(ok351)* *him-8(e1489)* male seam cell lineage trace is shown in Fig. 5D.

The most common lineage defect in *rnt-1* animals involves failures in L2 and L3 seam cell divisions. L1 divisions were

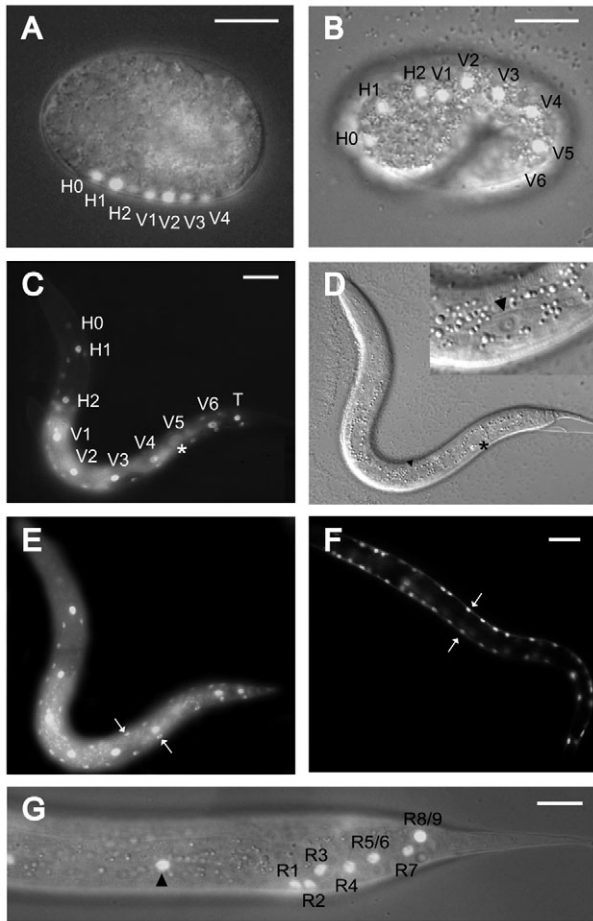


**Fig. 4.** Domains of expression of *rnt-1*. (A,B) *rnt-1(e1241); him-5(e1490)* embryos carrying a rescuing *rnt-1::GFP* reporter construct. (A) *rnt-1* expression is first seen in seam cell nuclei in embryos around 260 minutes after fertilisation. Dorsal view. Seam cells are visible on one side of the embryo (the left side) in this focal plane. Seven out of the nine H and V seam cells, labelled H0-H2 and V1-V4 are visible; V5 and V6 are out of focus. The T seam cell is ventral at this stage of development (Sulston et al., 1983). (B) Seam cell expression of *rnt-1::GFP* at the 1.5-fold stage. Lateral view. H and V seam cell nuclei are labelled. Again, T is out of focus, as is V6. Anterior is towards the left in both panels. Scale bar: 20  $\mu$ m. (C,D) Seam cell expression of *rnt-1::GFP* in L1 larvae. (C) Lateral view. Seam cell nuclei are labelled. V5 is dividing (asterisk). Expression in H0 is fainter than in the other seam cells. Scale bar: 20  $\mu$ m. (D) Corresponding Nomarski image. The outline of the dividing cell is clearly visible (asterisk). Inset is a higher magnification image of V3 (arrowhead) showing the morphology of seam cells. Anterior is towards the left in both panels. (E) Expression of *rnt-1::GFP* in body wall muscle nuclei. This is the same animal as in C, slightly different focal plane. Body wall muscle cells are present as four longitudinal rows at this stage, one ventral row and one dorsal row on each side of the animal. Two out of the four rows (one dorsal and one ventral) are visible in this lateral view (arrows). (F) *myo-3::GFP* body wall muscle reporter for comparison. Again, two longitudinal rows of cells are visible in this lateral view (arrows). Anterior is towards the left. Scale bar: 20  $\mu$ m. (G) Male tail expression of *rnt-1::GFP* in early L3 showing ray precursor cells R1-R9. R5/6 and R8/9 have yet to divide. The V5-derived cell labelled with an arrowhead forms part of the body seam. Posterior is towards the right. Scale bar: 20  $\mu$ m.

found to be normal in all animals analysed. Thus, the main role of *rnt-1* is to stimulate divisions of seam cells from L2 onwards. The lineage traces shown illustrate the variable nature of the division failures in different seam lineages. Moreover, different animals displayed different seam lineage failures (data not shown). This explains why *rnt-1* males end up with a variable number of missing rays. L4 divisions and male ray sublineages were not extensively lineaged. The lineage defects observed do not appear to be heterochronic alterations, as lineages are only partially affected (usually the posterior branch). Two examples of potential cell fate transformations (in the anterior branch of V1 in the hermaphrodite and in the posterior branch of T in the male) were observed, but this type of defect was found to be rare.

### Ectopic expression of *rnt-1* causes seam cell hyperplasia

Deregulated expression (both loss and gain of function) of Runx genes in humans is associated with various cancers (reviewed by Cameron and Neil, 2004). In particular, amplification of *Runx1* has been associated with leukaemia (Roumier et al., 2003). To test the effects of overexpressing *rnt-1* in *C. elegans*, we constructed transgenic worms carrying a full-length *rnt-1* cDNA driven by the heat shock promoter *hsp16-2*, which drives high level expression in seam, hypodermal and neuronal cells (see Materials and methods). We found that heat shock of transgenic worms prior to L2 or after L3 had no effect on adult seam cell number (as assayed by *scm::GFP* expression), but heat shock during L2 and L3 caused a significant increase in the number of seam cells present in adult hermaphrodites (Fig. 6), indicating that *rnt-1* is both necessary and sufficient for seam cell proliferation. Moreover, in males, these extra seam cells are capable of differentiating into extra rays (Fig. 6D).

Overexpression of *rnt-1* does not appear to cause hyperplasia in other cell types. We looked at the number of intestinal nuclei (using an *elt-2::GFP* intestinal reporter) in heat shocked worms carrying an *hsp16-41::rnt-1* construct (which would be expected to drive high level expression in the intestine) and found it to be normal (data not shown). We likewise found no increase in the number of body wall muscle cells, assayed using a *myo-3::GFP* reporter strain in heat shocked worms carrying an *hsp16-2::rnt-1* construct (data not shown).

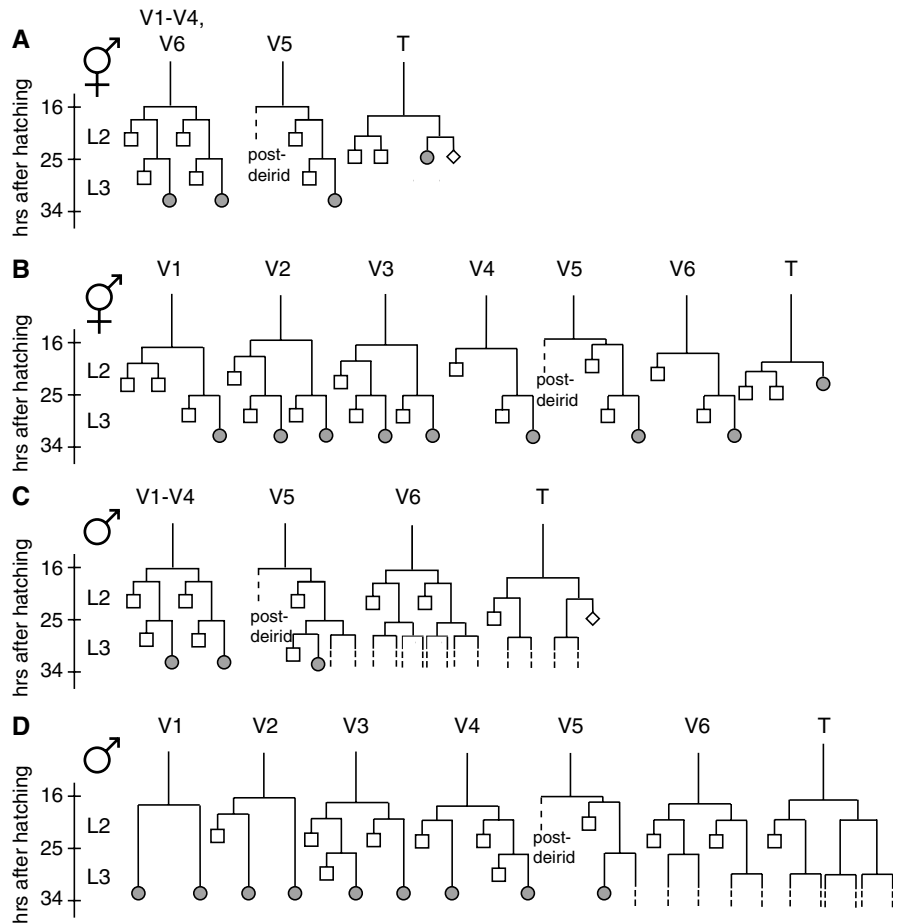
### Suppression of *rnt-1* seam cell division failures by *cki-1* RNAi

*cki-1* is a member of the KIP/CIP family of CDK inhibitors and is most similar to *p27/kip1*, which functions to link developmental programmes to cell cycle progression (Boxem and van den Heuvel, 2001; Fukuyama et al., 2003; Hong et al., 1998). KIP/CIP CDK inhibitors are thought to act by inhibiting the activity of the cyclin E/CDK2 complex during G1 (reviewed by Sherr, 2000). *cki-1* in *C. elegans* has been reported to be required for developmental cell cycle arrest in several lineages and is known to be expressed in seam cells (Fukuyama et al., 2003; Hong et al., 1998). The temporal pattern of *cki-1* expression in seam cells partially overlaps with that of *rnt-1*. Both genes are expressed strongly during embryogenesis and until mid-L1 (this report) (Fukuyama et al., 2003). High level expression of *rnt-1* persists during larval

**Fig. 5.** *rnt-1* is necessary for seam cell proliferation, not fate determination. Lineage traces are shown up to mid L3. The L1 asymmetric division is omitted for simplicity. Seam cells are indicated by circles, hyp7 nuclei by squares, and glial and neuronal cells by diamonds. Broken lines indicate incomplete lineages. The data shown are lineage traces for single animals. Five animals were lineage traced and found to give similar results. (A) Wild-type hermaphrodite V1-V6 and T lineages. (B) *rnt-1(ok351)* hermaphrodite lineage trace of V1-V6 and T divisions. V2 and V3 divisions display a similar pattern in the lineage trace shown; the anterior branch divides normally, but there is a failure of the L2 asymmetric division in the posterior branch, leading to a reduction in hypodermal nuclei. V4 and V6 display a different defect; this time the L2 proliferative division fails, causing a reduction in seam and hypodermal nuclei. V5 divisions are normal in this lineage trace, leading to the correct formation of the post-deirid neuroblast. Normal post-deirids appeared to be present in all *rnt-1* animals analysed (data not shown). V1 displays a similar defect to V2 and V3 in the posterior branch, a failure of the L2 asymmetric division, but there is an additional defect in the anterior branch. Both daughter nuclei from the L2 'asymmetric' division appear to fuse with the hypodermal syncytium, rather than the posterior daughter undergoing the proliferative fate. In the T lineage, the anterior branch is normal, but there is a division failure in the posterior branch, yielding just one seam cell, rather than a seam cell plus a glial cell. (C) Wild-type male V1-V4, V5, V6 and T lineages. A description of these divisions is given in the legend to Fig. 3. (D) *rnt-1(ok351); him-8(e1489)* male seam cell lineage trace. In V1 the L2 proliferative division occurs normally but there are no further divisions. Both daughters resemble seam cells. In V2, the posterior daughter of the L2 proliferative division does not divide further in L2 or L3 (it remains as a seam cell), while the anterior daughter undergoes one further asymmetric division in L2 to produce a hypodermal daughter and a seam daughter that fails to divide further in L3. In V3, the L2 proliferative division occurs normally and the anterior branch undergoes the normal asymmetric divisions in L2 and L3, while the posterior branch undergoes one asymmetric division in L2, after which the posterior seam daughter fails to divide further. In V4, the L2 proliferative division occurs normally and the anterior branch displays a similar division pattern to the anterior branch of V2, while the posterior branch undergoes the normal L2 and L3 asymmetric divisions. In V5, the anterior branch is normal but the posterior branch fails after the first L3 proliferative division, with both daughters failing to divide. In V6, L2 divisions are normal but there are failures in L3 divisions. The wild-type male V6 lineage normally undergoes two rounds of division in early L3, whereas in this *rnt-1* male, only one round of division occurs in each branch. In the T lineage, the anterior branch was normal but there was, unusually, an extra proliferative division in the posterior branch during L2.

development, whereas *cki-1* expression declines sharply at mid-L1, to be restored during resting phases between larval moults and at L4, coincident with seam cell terminal differentiation (Fukuyama et al., 2003).

To test for a genetic interaction between *rnt-1* and *cki-1*, we removed *cki-1* expression by RNAi in a *rnt-1* mutant background and assayed seam cell number. *cki-1* RNAi in wild-type worms causes an increase in seam cell number in treated animals which survive to adulthood (Fig. 7A), indicating that *cki-1* normally acts to limit seam cell proliferation. This is in agreement with a previous report showing seam cell hyperplasia induced by *cki-1* RNAi in embryos (Fukuyama et al., 2003). When *rnt-1(ok351)* animals (which normally have reduced seam cell proliferation) are subjected to *cki-1* RNAi, adult seam cell number is restored to almost wild-type levels (Fig. 7A). This suggests that *rnt-1* and



*cki-1* may act at a similar point in the cell cycle to control seam cell proliferation in opposing ways.

One model for the opposing roles of *rnt-1* and *cki-1* in controlling seam cell proliferation would be that RNT-1 negatively regulates *cki-1* expression in seam cells. We tested this possibility by examining *cki-1::GFP* expression in a *rnt-1* mutant. The best situation in which *cki-1* expression could be robustly analysed in seam cells during larval development was found to be during L1 (we found *cki-1::GFP* reporter expression to be too faint to analyse reliably after L1). Although, as discussed above, loss of *rnt-1* does not normally affect the L1 stem cell division, we found that this division fails in *rnt-1* animals that have been arrested in L1 diapause by hatching in the absence of food, before being allowed to recommence larval development by introducing food (Fig. 7B). By contrast, wild-type animals undergo this division normally

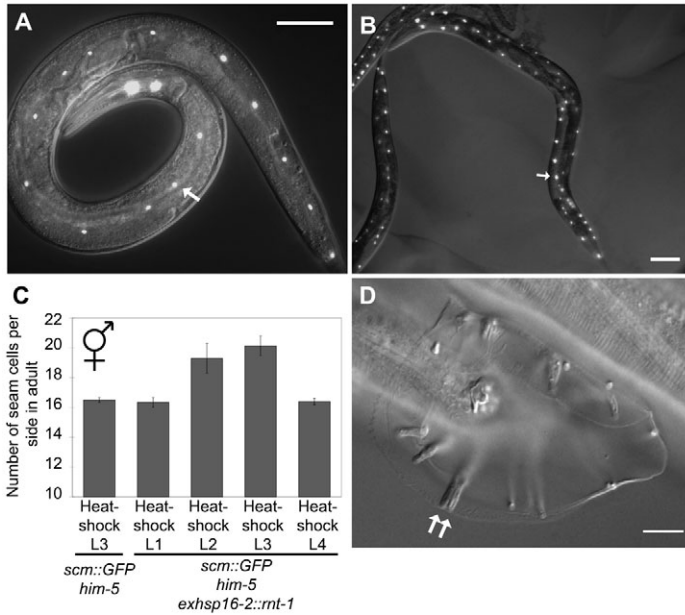


**Fig. 6.** Overexpression of *rnt-1* drives extra seam cell divisions. (A) Control wild-type worms subjected to heat shock (33°C, 1 hour) have the normal number of seam cells, visualised in adults with the *scm::GFP* reporter (white arrow). Scale bar: 70  $\mu$ m. (B) Adult hermaphrodite carrying the *hsp16-2::rnt-1* construct, previously subjected to heat shock (33°C, 1 hour) in L3. Several extra seam cells are visible with the *scm::GFP* reporter (white arrow). Anterior is towards the left in both panels. Scale bar: 70  $\mu$ m. (C) Graph showing a quantitative analysis of adult seam cell number in heat shocked worms. Wild-type hermaphrodites subjected to heat shock (33°C, 1 hour) during L2 or L3 have the normal adult number of seam cells (data not shown). Transgenic worms carrying the *hsp16-2::rnt-1* construct display the normal adult seam cell number following no heat shock ( $n=30$ ), or heat shock during L1 ( $n=42$ ) or L4 ( $n=25$ ), but have extra seam cells following heat shock during L2 ( $n=31$ ,  $P<0.01$ ) or L3 ( $n=48$ ,  $P<0.00001$ ). Error bars represent the standard error of the mean. (D) *him-5(e1490)* male carrying the *hsp16-2::rnt-1* construct. This animal had been previously subjected to heat shock during L2. An extra ray 3 is visible on one side of the animal, fused to the expected single ray 3 (white arrows). Scale bar: 10  $\mu$ m

when subjected to the same treatment (Fig. 7B), i.e. starvation sensitises the L1 division to loss of *rnt-1*. As shown in Fig. 7B, we found that *cki-1::GFP* expression in *rnt-1* mutants whose seam cells fail to divide in L1 is higher than in wild-type animals whose seam cells divide normally. In other words, division failure is correlated with increased *cki-1::GFP* expression. This is good evidence that *rnt-1* normally acts during G1 of the cell cycle to promote cell division by somehow downregulating *cki-1* expression. It is not clear at present whether this interaction is direct or indirect.

## Discussion

### *rnt-1* promotes seam cell proliferation

All alleles of *rnt-1* examined display similar male tail abnormalities owing to the loss of V and T lineage-derived rays. The cellular basis of the ray loss phenotype is a reduction in seam cell proliferation during larval development. Our data suggest that *rnt-1* is required for both the proliferative and asymmetric divisions of seam cells that occur in males and hermaphrodites. In males, the cumulative effect of V5, V6 and T lineage divisions is to produce the correct number of ray precursor cells and execute the correct ray sublineages, hence *rnt-1* mutants have missing rays. We found that silencing of *cki-1*, a G1 inhibitor normally active in seam cells, suppresses the seam cell proliferation defect, suggesting that *rnt-1* and *cki-1* act on the cell cycle to regulate cell proliferation in opposing ways. Intriguingly, we found that *cki-1::GFP* seam cell expression is upregulated in *rnt-1* mutants, suggesting that RNT-1 acts in G1 to promote seam cell divisions *via* the downregulation of *cki-1*.

Our data support the view that the loss of seam cells is mainly the result of a defect in cell proliferation *per se*, rather than a change in cell fate. The rare cell fate, as opposed to cell proliferation, defects we did observe in *rnt-1* animals may be explained by signalling defects. It is known that signalling among seam cells (acting in conjunction with lineage cues) is important for cell fate determination. This has been

demonstrated most clearly in ablation studies, where extensive ablation of seam cells was found to cause various cell fate changes in the remaining seam cells (Sulston and White, 1980). Thus, cells with inappropriate neighbours may be expected to take on the wrong fate under certain circumstances. In this context, it becomes somewhat artificial to postulate a clear distinction between cell proliferation and cell fate determination.

A recent report suggests that *rnt-1* functions to regulate body size and ray morphogenesis in *C. elegans* by interacting with components of the Sma/Mab TGF $\beta$  signalling pathway (Ji et al., 2004). Although we do observe a small (5%) decrease in length in *rnt-1* adult hermaphrodites, this is much less severe than in Sma animals. In the case of *rnt-1*, we suggest that this slight reduction in size is caused by a reduction in the number of nuclei in the hypodermal syncytium, which is caused by seam cell division failures. The relationship between hypodermal ploidy and body size in *C. elegans* has been previously discussed (Flemming et al., 2000). Moreover, we can see no phenotypic similarities between *rnt-1* and Sma male tails. The Sma phenotype is typified by fused rays (Hodgkin, 1983; Morita et al., 1999; Savage-Dunn et al., 2003), whereas the *rnt-1* phenotype is typified by missing rays caused by failures in seam cell proliferation, as indicated by our lineage analysis. It is possible that *rnt-1* has some minor downstream role in ray morphogenesis, as evidenced by the very low penetrance ray fusion phenotype we observe in *rnt-1* animals, but it is certain that the major focus of *rnt-1* action is in the regulation of seam cell proliferation. Given that missing rays are not observed in Sma mutants, we consider it unlikely that this major function of *rnt-1* involves an interaction with the Sma/Mab TGF $\beta$  pathway.

Other genes known to influence ray development tend to affect specific ray sublineages. For example, *mab-5*, a posterior Hox gene, is required for proliferation and ray production in V5 and V6 sublineages but does not affect T lineage-derived rays (Kenyon, 1986; Salser and Kenyon, 1996). By contrast, ray loss in *mab-19* mutants is restricted to

T lineage-derived rays (Sutherland and Emmons, 1994). *rnt-1*, however, has a more general role in seam cell proliferation which is required for the subsequent development of both V and T-derived rays.

Defective male tail formation is the only highly penetrant gross morphological phenotype associated with loss of *rnt-1* function, and consistent with this we found seam cells, and ray sublineage cells in the male, to be the major focus of *rnt-1* expression. However, we did notice a low level of embryonic lethality associated with *rnt-1* RNAi and in the presumed null allele *os58*. The reason for this low level of embryonic lethality is not clear. Perhaps *rnt-1* acts partially redundantly with some other factor in embryos. We also found *rnt-1* to be transiently expressed in body wall muscle nuclei from late embryogenesis until the end of L2, but this expression does not appear to be associated with any obvious muscle function. Using a rescuing GFP reporter construct, we did not see *rnt-1* expression in any

other cell type. In particular, we did not see expression in hyp7 nuclei, suggesting that *rnt-1* expression is switched off in cells derived from the seam, whose fate is to fuse with hyp7, and therefore to stop dividing.

### *rnt-1* overexpression drives ectopic cell divisions

Loss of *rnt-1* function is associated with a failure of seam cell proliferation, whereas overexpression of *rnt-1* drives seam cell hyperplasia, indicating that *rnt-1* can function as a rate-limiting regulator of cell proliferation. It is noteworthy that seam cell hyperplasia occurs only if *rnt-1* is overexpressed in L2 or L3. This is consistent with the normal expression pattern of *rnt-1* in seam cells becoming fainter from L2 onwards, suggesting that seam cell lineages may not be able to cope with high level *rnt-1* expression after this stage. High level expression during L2 and L3 is therefore sufficient to drive inappropriate cell divisions, leading to seam cell hyperplasia. Perhaps during L4 there are other constraints on cell proliferation, rendering seam cells recalcitrant to high-level *rnt-1* expression during late larval development.

Overexpression of *rnt-1* was not found to be associated with hyperplasia in other cell types. The tissue and stage specificity of RNT-1-induced hyperplasia suggests that the ability of RNT-1 to drive cell proliferation may be limited by the expression of some co-factor or of some other proliferation 'licensing factor'. Runx genes have been shown to associate with a binding partner, *CBFβ*, in other species (reviewed by Coffman, 2003). An orthologue of *CBFβ*, *bro-1*, exists in *C. elegans*, but the function and expression pattern of this subunit has not yet been reported. Perhaps if *rnt-1* and *bro-1* were co-expressed, more widespread hyperplasia would result.

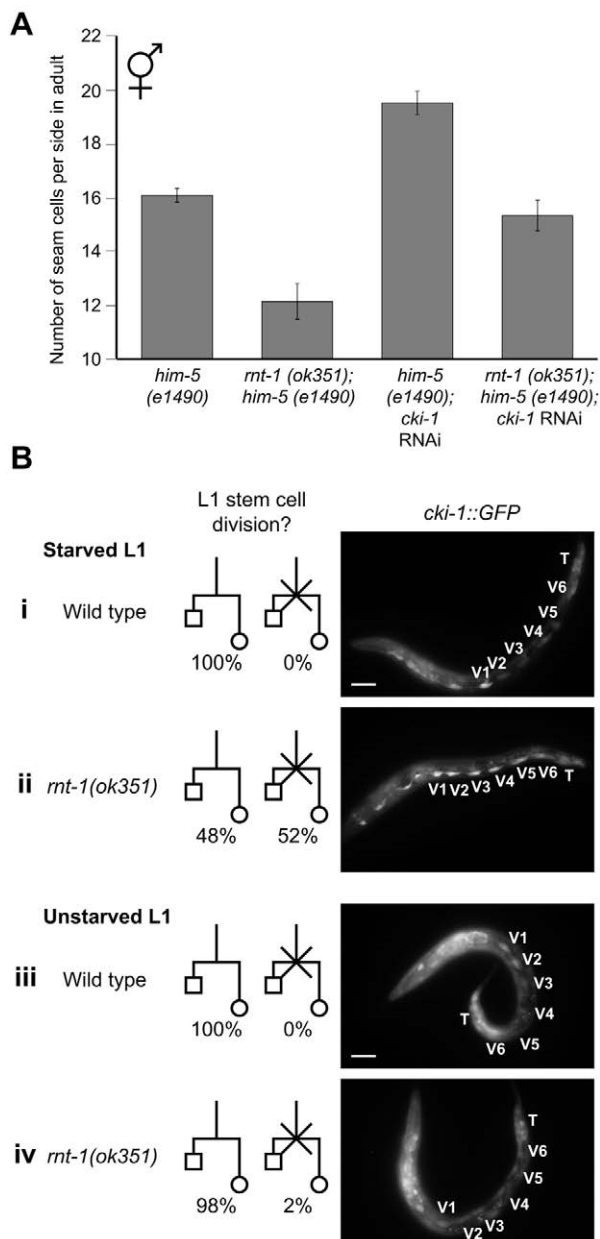


**Fig. 7.** Suppression of *rnt-1* cell division failures by silencing of *cki-1*. (A) Graph showing the number of seam cells present in adult hermaphrodites (assayed by *scm::GFP* expression) in wild-type ( $n=30$ ), *rnt-1(ok351)* ( $n=32$ ), *cki-1(RNAi)* ( $n=36$ ) and *rnt-1(ok351); cki-1(RNAi)* ( $n=31$ ) animals. All strains were in a *him-5(e1490)* background. *cki-1* RNAi causes an increase in seam cell number relative to wild type ( $P<0.0001$ ). The number of seam cells in *rnt-1(ok351); cki-1(RNAi)* animals is restored to near wild-type levels (no significant difference compared with wild type,  $P>0.05$ ). Error bars represent the standard error of the mean. (B) *cki-1::GFP* expression in the seam cells of L1 larvae. The left hand panel shows the L1 stem cell division pattern of V1-V6 in wild-type and *rnt-1(ok351)* animals. Seam cells are indicated by circles, hyp7 nuclei by squares. Crosses in the lineage diagrams indicate where divisions failed. (i,ii) Worms hatched in the absence of food, kept 24 hours at 20°C then re-fed and the division pattern examined by observing hypodermal and seam nuclei present in late L1 or mid L2 stages. In this situation, the L1 stem cell division failed in *rnt-1* mutants 52% of the time ( $n=84$ ). In wild type, the division pattern was always normal ( $n=66$ ). (iii,iv) Worms were examined in late L1 after hatching on food, having never been subjected to starvation. Wild-type animals always underwent the normal L1 division ( $n=60$ ) and *rnt-1(ok351)* animals displayed the normal division pattern 98% of the time ( $n=60$ ). The right-hand panel shows *cki-1::GFP* expression under these conditions, prior to the time of the expected L1 stem-cell division. Individual seam cells are labelled. The increased *cki-1::GFP* expression observed in *rnt-1* L1 larvae hatched in the absence of food, compared with wild-type animals subjected to the same treatment, was consistently observed ( $n=30$ ). Scale bars: 20  $\mu$ m.

## Conservation of Runx function

Runx genes have previously been characterised from a variety of metazoan organisms (reviewed by Coffman, 2003). In mammals there are three members of the family and they appear to have lineage-specific functions. *Runx1* (also known as *AML1*, *PEBP2 $\alpha$ B* and *CBFA2*) is required for definitive haematopoiesis (reviewed by Okuda et al., 2001). Recently, it has also been shown that *Runx1* is required for the proliferation of early developing thymocytes (Sato et al., 2003). Clinically, *Runx1* is strongly associated with human leukaemia. Indeed, *Runx1* is one of the genes most frequently deregulated in leukaemia through different mechanisms involving translocation, mutation and amplification (reviewed by Roumier et al., 2003). *Runx1* has been shown to actively drive cultured mammalian cells from G1 into S phase (Strom et al., 2000), and overexpression of *Runx1* in NIH3T3 cells has been reported to lead to neoplastic transformation (Kurokawa et al., 1996). *Runx1* has been regarded in the literature both as a tumour suppressor and as a proto-oncogene (Cameron and Neil, 2004; Coffman, 2003).

An intriguing link between the function of *rnt-1* in *C. elegans* seam cells and the function of *Runx1* in haematopoiesis is that both of these developmental lineages have stem cell-like properties: relatively undifferentiated cells continue dividing (self renewal), throwing off daughter cells that can undergo terminal differentiation into particular cell types. Perhaps a particular kind of signal, involving Runx genes, must be generated in stem cell-like lineages to promote proliferation.

*Runx2* and *Runx3* also appear to function in developmental lineages with stem cell-like properties. *Runx2*<sup>-/-</sup> mice fail to undergo osteogenesis, dying shortly after birth (Komori et al., 1997; Otto et al., 1997). In humans, *Runx2* (also known as *Cbfa1*) is commonly associated with the congenital bone malformation cleidocranial dysplasia (Otto et al., 2002). *Runx3* is required in mice for neurogenesis of the dorsal root ganglia (Inoue et al., 2002; Levanon et al., 2002). *Runx3* has also been reported to be involved in controlling growth of the gastric epithelium in mice, and has been associated with human gastric cancers where it appears to act as a tumour suppressor gene (Li et al., 2002).

Overall, it has been suggested that Runx genes are required to maintain the balance between cell proliferation and differentiation in a variety of developmental contexts (reviewed in Coffman, 2003). One of the most important controls concerns the regulation of cell number. Too few cells in a given lineage and formation of a particular structure will not be possible, too many cells and an aberrant structure or a tumour may form. *rnt-1* in *C. elegans* is part of the control that ensures developmental outputs are composed of the appropriate number of cells. In other systems, deregulated cell proliferation is at the heart of carcinogenesis.

It is noteworthy that the *C. elegans* genome contains only one Runx gene, whereas most other genomes so far examined contain multiple Runx orthologues. This makes *C. elegans* an organism of choice for the further study of this important family of transcription factors. Perhaps *rnt-1* in *C. elegans* represents the primitive Runx function, promoting cell proliferation in developmental lineages where choices must be continually made between proliferative and differentiative division patterns.

We thank Hitoshi Sawa (Kobe, Japan) and Hiroshi Kagoshima (Shizuoka, Japan) for sharing alleles and information prior to publication. We also thank the Caenorhabditis Genetics Center (Minneapolis, USA) and the *C. elegans* KO Consortium (Oklahoma, USA) for sending strains. This work was funded by the UK Medical Research Council and the Association for International Cancer Research.

## References

- Boxem, M. and van den Heuvel, S.** (2001). lin-35 Rb and cki-1 Cip/Kip cooperate in developmental regulation of G1 progression in *C. elegans*. *Development* **128**, 4349-4359.
- Cameron, E. R. and Neil, J. C.** (2004). The Runx genes: lineage-specific oncogenes and tumor suppressors. *Oncogene* **23**, 4308-4314.
- Coffman, J. A.** (2003). Runx transcription factors and the developmental balance between cell proliferation and differentiation. *Cell. Biol. Int.* **27**, 315-324.
- Fire, A., Xu, S., Montgomery, M. K., Kostas, S. A., Driver, S. E. and Mello, C. C.** (1998). Potent and specific genetic interference by double-stranded RNA in *Caenorhabditis elegans* [see comments]. *Nature* **391**, 806-811.
- Flemming, A. J., Shen, Z. Z., Cunha, A., Emmons, S. W. and Leroy, A. M.** (2000). Somatic polyploidization and cellular proliferation drive body size evolution in nematodes. *Proc. Natl. Acad. Sci. USA* **97**, 5285-5290.
- Fukuyama, M., Gendreau, S. B., Derry, W. B. and Rothman, J. H.** (2003). Essential embryonic roles of the CKI-1 cyclin-dependent kinase inhibitor in cell-cycle exit and morphogenesis in *C. elegans*. *Dev. Biol.* **260**, 273-286.
- Hodgkin, J.** (1983). Male phenotypes and mating efficiency in *Caenorhabditis elegans*. *Genetics* **103**, 43-64.
- Hong, Y., Roy, R. and Ambros, V.** (1998). Developmental regulation of a cyclin-dependent kinase inhibitor controls postembryonic cell cycle progression in *Caenorhabditis elegans*. *Development* **125**, 3585-3597.
- Inoue, K., Ozaki, S., Shiga, T., Ito, K., Masuda, T., Okado, N., Iseda, T., Kawaguchi, S., Ogawa, M., Bae, S. C. et al.** (2002). Runx3 controls the axonal projection of proprioceptive dorsal root ganglion neurons. *Nat. Neurosci.* **5**, 946-954.
- Ji, Y. J., Nam, S., Jin, Y. H., Cha, E. J., Lee, K. S., Choi, K. Y., Song, H. O., Lee, J., Bae, S. C. and Ahn, J.** (2004). RNT-1, the *C. elegans* homologue of mammalian RUNX transcription factors, regulates body size and male tail development. *Dev. Biol.* **274**, 402-412.
- Kamath, R. S., Fraser, A. G., Dong, Y., Poulin, G., Durbin, R., Gotta, M., Kanapin, A., Le Bot, N., Moreno, S., Sohrmann, M. et al.** (2003). Systematic functional analysis of the *Caenorhabditis elegans* genome using RNAi. *Nature* **421**, 231-237.
- Kenyon, C.** (1986). A gene involved in the development of the posterior body region of *C. elegans*. *Cell* **46**, 477-487.
- Komori, T., Yagi, H., Nomura, S., Yamaguchi, A., Sasaki, K., Deguchi, K., Shimizu, Y., Bronson, R. T., Gao, Y. H., Inada, M. et al.** (1997). Targeted disruption of *Cbfa1* results in a complete lack of bone formation owing to maturational arrest of osteoblasts. *Cell* **89**, 755-764.
- Kurokawa, M., Tanaka, T., Tanaka, K., Ogawa, S., Mitani, K., Yazaki, Y. and Hirai, H.** (1996). Overexpression of the AML1 proto-oncoprotein in NIH3T3 cells leads to neoplastic transformation depending on the DNA-binding and transactivational potencies. *Oncogene* **12**, 883-892.
- Levanon, D., Bettoun, D., Harris-Cerruti, C., Woolf, E., Negreanu, V., Eilam, R., Bernstein, Y., Goldenberg, D., Xiao, C., Fliegauf, M. et al.** (2002). The Runx3 transcription factor regulates development and survival of TrkC dorsal root ganglia neurons. *EMBO J.* **21**, 3454-3463.
- Li, Q. L., Ito, K., Sakakura, C., Fukamachi, H., Inoue, K., Chi, X. Z., Lee, K. Y., Nomura, S., Lee, C. W., Han, S. B. et al.** (2002). Causal relationship between the loss of RUNX3 expression and gastric cancer. *Cell* **109**, 113-124.
- Mello, C. and Fire, A.** (1995). DNA transformation. In *Caenorhabditis elegans: Modern Biological Analysis of an Organism*, Vol. 48 (ed. D. Shakes and H. Epstein), pp. 451-482. London: Academic Press.
- Morita, K., Chow, K. L. and Ueno, N.** (1999). Regulation of body length and male tail ray pattern formation of *Caenorhabditis elegans* by a member of TGF-beta family. *Development* **126**, 1337-1347.
- Nam, S., Jin, Y. H., Li, Q. L., Lee, K. Y., Jeong, G. B., Ito, Y., Lee, J. and Bae, S. C.** (2002). Expression pattern, regulation, and biological role of runt domain transcription factor, run, in *Caenorhabditis elegans*. *Mol. Cell. Biol.* **22**, 547-554.
- Okuda, T., Nishimura, M., Nakao, M. and Fujita, Y.** (2001).

- RUNX1/AML1: a central player in hematopoiesis. *Int. J. Hematol.* **74**, 252-257.
- Otto, F., Thornell, A. P., Crompton, T., Denzel, A., Gilmour, K. C., Rosewell, I. R., Stamp, G. W., Beddington, R. S., Mundlos, S., Olsen, B. R. et al.** (1997). Cbfa1, a candidate gene for cleidocranial dysplasia syndrome, is essential for osteoblast differentiation and bone development. *Cell* **89**, 765-771.
- Otto, F., Kanegane, H. and Mundlos, S.** (2002). Mutations in the RUNX2 gene in patients with cleidocranial dysplasia. *Hum. Mutat.* **19**, 209-216.
- Roumier, C., Fenaux, P., Lafage, M., Imbert, M., Eclache, V. and Preudhomme, C.** (2003). New mechanisms of AML1 gene alteration in hematological malignancies. *Leukemia* **17**, 9-16.
- Salser, S. J. and Kenyon, C.** (1996). A *C. elegans* Hox gene switches on, off, on and off again to regulate proliferation, differentiation and morphogenesis. *Development* **122**, 1651-1661.
- Sato, T., Ito, R., Nunomura, S., Ohno, S., Hayashi, K., Satake, M. and Habu, S.** (2003). Requirement of transcription factor AML1 in proliferation of developing thymocytes. *Immunol. Lett.* **89**, 39-46.
- Savage-Dunn, C., Maduzia, L. L., Zimmerman, C. M., Roberts, A. F., Cohen, S., Tokarz, R. and Padgett, R. W.** (2003). Genetic screen for small body size mutants in *C. elegans* reveals many TGFbeta pathway components. *Genesis* **35**, 239-247.
- Sherr, C. J.** (2000). The Pezcoller lecture: cancer cell cycles revisited. *Cancer Res.* **60**, 3689-3695.
- Strom, D. K., Nip, J., Westendorf, J. J., Linggi, B., Lutterbach, B., Downing, J. R., Lenny, N. and Hiebert, S. W.** (2000). Expression of the AML-1 oncogene shortens the G(1) phase of the cell cycle. *J. Biol. Chem.* **275**, 3438-3445.
- Sulston, J. E. and Horvitz, H. R.** (1977). Post-embryonic cell lineages of the nematode, *Caenorhabditis elegans*. *Dev. Biol.* **56**, 110-156.
- Sulston, J. E. and White, J. G.** (1980). Regulation and cell autonomy during postembryonic development of *Caenorhabditis elegans*. *Dev. Biol.* **78**, 577-597.
- Sulston, J. and Hodgkin, J.** (1988). Methods. In *The Nematode Caenorhabditis elegans* (ed. W. B. Wood), pp. 587-606. New York: Cold Spring Harbor Laboratory Press.
- Sulston, J. E., Albertson, D. G. and Thomson, J. N.** (1980). The *Caenorhabditis elegans* male: postembryonic development of nongonadal structures. *Dev. Biol.* **78**, 542-576.
- Sulston, J. E., Schierenberg, E., White, J. G. and Thomson, J. N.** (1983). The embryonic cell lineage of the nematode *Caenorhabditis elegans*. *Dev. Biol.* **100**, 64-119.
- Sutherlin, M. E. and Emmons, S. W.** (1994). Selective lineage specification by mab-19 during *Caenorhabditis elegans* male peripheral sense organ development. *Genetics* **138**, 675-688.
- Williams, B. D.** (1995). Genetic mapping with polymorphic sequence-tagged sites. In *Caenorhabditis elegans: Modern Biological Analysis of an Organism*, Vol. 48 (ed. D. Shakes and H. Epstein), pp. 81-96. London: Academic Press.
- Zhu, L. and Skoultschi, A. I.** (2001). Coordinating cell proliferation and differentiation. *Curr. Opin. Genet. Dev.* **11**, 91-97.